# FATIGUE BEHAVIOR OF API GRADE 5L X-65 AND X-70 STEELS WELDED JOINTS UNDER VARIABLE AMPLITUDE LOADING

**Beltrão, M. A. N**
Federal University of Rio de Janeiro (UFRJ), Metallurgical and Materials Engineering Program (PEMM)
Technological Center, Bl. F/210, CEP 21949-900, Rio de Janeiro, RJ, Brazil
beltrao@metalmat.ufrj.br

**Castrodeza, E. M**
Federal University of Rio de Janeiro (UFRJ), Metallurgical and Materials Engineering Program (PEMM)
castrode@metalmat.ufrj.br

**de Marco Filho, Flávio**
Federal University of Rio de Janeiro (UFRJ), Mechanical Engineering Department - DEM/POLI
flavio@mecanica.coppe.ufrj.br

**Bastian, Fernando Luiz**
Federal University of Rio de Janeiro (UFRJ), Metallurgical and Material Engineering Program - PEMM/COPPE
fbastian@metalmat.ufrj.br

***Abstract***. *The fatigue behavior of base metal, weld metal and heat affected zone (HAZ) of circumferential and longitudinal welded joints of API 5L X-65 and API 5L X-70 pipeline steels, respectively, used in oil and gas transportation were studied. Variable amplitude fatigue tests were carried under load control for R = 0.1 and 0.5 with application of tensile overloads (50 and 100% of maximum load) at API 5L X-65 steel welded joints and alternate tensile overloads at 2,5mm crack growth intervals (75 and 100% of maximum load) at API 5L X-70 steel welded joints. The fatigue tests results were obtained as da/dN vs.ΔK curves. It could be inferred from these curves that for R = 0.1 the weld metal and HAZ showed similar behavior whereas the welded joints of API 5L X-70 steel showed the greatest crack growth rates for R = 0.5. It was observed that the delay on the fatigue crack growth of welded joints of API 5L X-70 decreased with the increase of ΔK.*

***Keywords***. *Fatigue, Crack Propagation, Welded Joints, Pipeline Steel, Overloads.*

## 1 – Introduction

The world increasing use of oil and gas is the main reason for the fast growth of research to improve pipeline steel properties. The properties usually required are high mechanical strength and toughness which are obtained by controlling factors like chemical composition, manufacturing process and final microstructure (Zhao *et al.*, 2002). These properties are also required in the welded joints of these materials.

Among materials that best respond to these requirements are HSLA steels (high-strength low-alloy). They are the result of optimal alloy selection, like Nb, Ti and V content, and controlled processing such as hot rolling. The HSLA steels used in this work are API X-65 and API X-70.

Despite their good mechanical properties when in operation the pipes are normally subjected to cyclic loads and after a period of service they can collapse by fatigue failure. The pipeline welded joints are prefered regions to start a fatigue crack because of the stress concentration effects caused by all sort of weld flaws. Nevertheless, when subjected to variable amplitude loading, the fatigue crack growth behavior can change. In this way, load interactions like overloads can promote delays on fatigue crack growth.

The work presented here is focused to compare the fatigue crack propagation behavior of the three regions of the welded joint, the base metal (BM), the weld metal (WM) and the heat affected zone (HAZ) at two stress ratios, $R$ = 0.1 and 0.5 of the circumferential, API X-65, and longitudinal, API X-70, welded joints, based on fracture mechanics concepts, under variable amplitude load.

## 2 – Experimental

### 2.1 - Materials

Circumferential and longitudinal welded joints of API 5L X-65 and X-70 pipeline steels, respectively, were studied in this research. Their chemical compositions are presented in tables 1 and 2, below.

Table 1. Chemical composition of pipeline steel API 5L X-65 (% of weight)

| C | Si | Mn | P | S | Al | Ni | Cu | Cr | Nb | Ti | N | $C_{eq}$ |
|---|---|---|---|---|---|---|---|---|---|---|---|---|
| 0.13 | 0.15 | 1.6 | 0.02 | 0.005 | 0.018 | 0.02 | 0.011 | 0.029 | 0.035 | 0.015 | 0.058 | 0,411 |

Table 2. Chemical composition of pipeline steel API 5L X-70 (% of weight)

| C | S | Al | Si | P | Ti | V | Cr | Mn | Ni | Cu | Nb | Mo | $C_{eq}$ |
|---|---|---|---|---|---|---|---|---|---|---|---|---|---|
| 0.08 | 0.002 | 0.028 | 0.25 | 0.017 | 0.027 | 0.045 | 0.02 | 1.73 | 0.194 | 0.016 | 0.064 | 0.003 | 0.40 |

These API 5L grade X-65 and X-70 steels are used for the fabrication of oil and gas pipelines and rigid risers. The specimens were cut from circumferential (X-65) and longitudinal (X-70) welded joints.

The microstructure of the three regions of both steels welded joints was characterized by optical microscopy. The process started with surface polishing followed by chemical etching with Nital 2%.

The weld process of the circumferential butt welds was the Gas Metal Arc Welding (GMAW) automatic. The main characteristics of the welding process are shown in table 3.

Table 3. Main characteristics of the welding procedure.

| **Electrode** | **Welding Conditions (average values per pass)** |
|---|---|
| Manufacturer: LINCOLN<br>Diameter [mm] = 1.0<br>Type of mixture: air/$CO_2$ – 50/50 | Current [A] = 229<br>Tension [V] = 24.7<br>Welding speed [cm/min] = 70<br>Heat input [kJ/cm] = 5.0 |

**2.2 – Fatigue tests**

Fatigue crack propagation tests of the circumferential and longitudinal welded joints were done using three point bending specimens (SE(B)) with square and rectangular sections, respectively. Longitudinal welded joint specimens were designed according to standard BS 6835 (figure 1A). However, due to the small pipe thickness in the case of steel X-65 their specimens were smaller than the standard recommendations (figure 1B). Although these dimensions were smaller than the recommended they have some interesting advantages, as reproducing the thickness of the real pipes from which the specimen were cut. According to Maddox (1998) this gives the tests conditions closer to the real ones and a greater reliability for the results.

The three point fatigue crack propagation tests were carried out according to the BS 6835 and ASTM E647 standards, under general conditions below. The dimensions of specimens are presented in table 4

- Senoidal load;
- Variable amplitude;
- Specimen: *Single Edge* - *Bending* - SE(B),
- Orientation L-R;
- Frequency = 30 Hz;
- $R$ = 0.1 and 0.5;
- Mean temperature ≈ 20$^o$ C;
- Ambient: air;
- Relative humidity of the air ≈ 60%.

Table 4. Dimensions of SE(B) specimens

| **Material** | **B (mm)** | **W (mm)** | **Notch (mm)** | **Pre-cracking (mm)** |
|---|---|---|---|---|
| API 5L X-65 | 12.5 | 12.5 | 6.0 | 0.8 |
| API 5L X-70 | 20.0 | 40.0 | 8.0 | 2.0 |

The values of $\Delta K$ used in this work were determined according to the function described in ASTM E399 standard which guarantees that crack propagation will always occur in the linear elastic region. The functions for API 5L X-65 and API 5L X-70 steels are shown below in equation 1 and 2, respectively.

$$\Delta K = \left(\sigma \cdot \sqrt{\pi a}\right) \cdot f\left(a/w\right) \tag{1}$$

where $$f\left(a/w\right) = \frac{\left(a/w\right)^{0,5} \cdot \left\{1.99 - \left(a/w\right) \cdot \left[1 - \left(a/w\right)\right]^2 \cdot \left[2.15 - 3.93 \cdot \left(a/w\right) + 2.7 \cdot \left(a/w\right)^2\right]\right\}}{\left(1 + 2a/w\right) \cdot \left(1 - a/w\right)^{1,5}}$$

$$\Delta K = \frac{\Delta PS}{BW^{1,5}} \cdot \left| \frac{3(a/W)^{0,5}\left[1,99 - (a/W)(1 - a/W)(2,15 - 3,93a/W + 2,7a^2/W^2)\right]}{2(1 + 2a/W)(1 - a/W)^{1,5}} \right| \tag{2}$$

For the welded joints of API X-70 steel, the application of overloads (75 and 100% of maximum load) was done in each 2.5mm of crack growth, avoiding any effect of interaction among overloads. The last overload of 100% was not applied on the specimens tested at $R = 0.5$, avoiding the specimen fracture. For the welded joints of API X-65 steel, the overload (50 and 100% of maximum overload) was applied at a crack growth equivalent to $\Delta K = 15$ MPa.m$^{0.5}$.

Parallel horizontal marks etched equally spaced of 0.38 mm for API X-65 and 0.5 mm for API X-70 steel, were previously made on the surface of the specimens for visual control and inspection. The measurement system used was an optical microscope to follow and measure crack growth.

Measurement of the increase in the crack length, $\Delta a$, the maximum and minimum loads, $\Delta P(a)$, and the corresponding number of cycles were recorded. Based on these values the fatigue crack propagation rate curves *(da/dN vs. ΔK)* were plotted out using logarithm scale. The polynomial method recommended by ASTM E647 standard was used.

## 3 – Results and discussion

### 3.1 – Metallographic analysis

The metallographic aspects of the three welded joint regions of the studied steels are presented in the figures below.

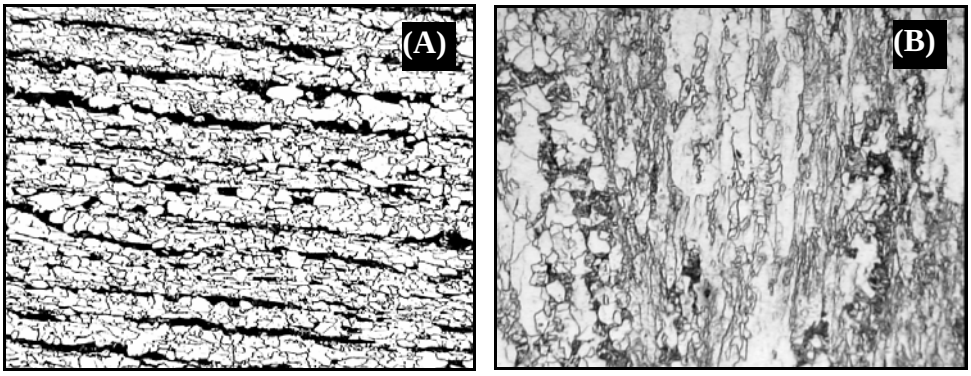


Figure 1. Microscope view of the base metal region of the steel (A) API X-65 and (B) API X-70 (200x).

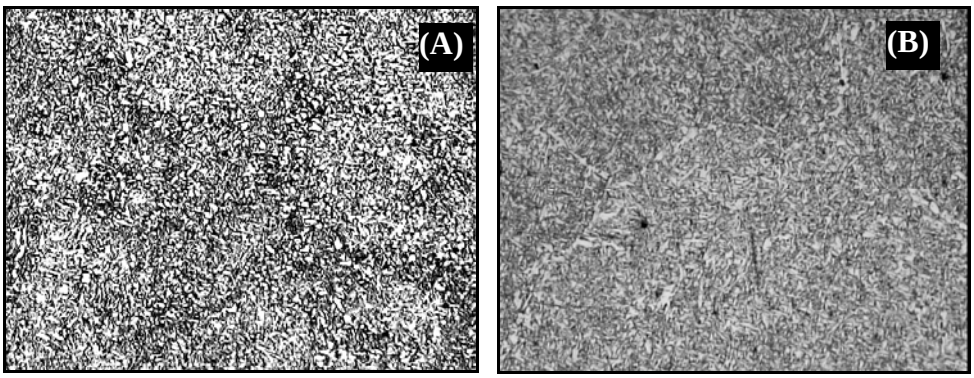


Figure 2. Microscope view of the welded metal region of the steel (A) API X–65 and (B) API X–70 (200x).

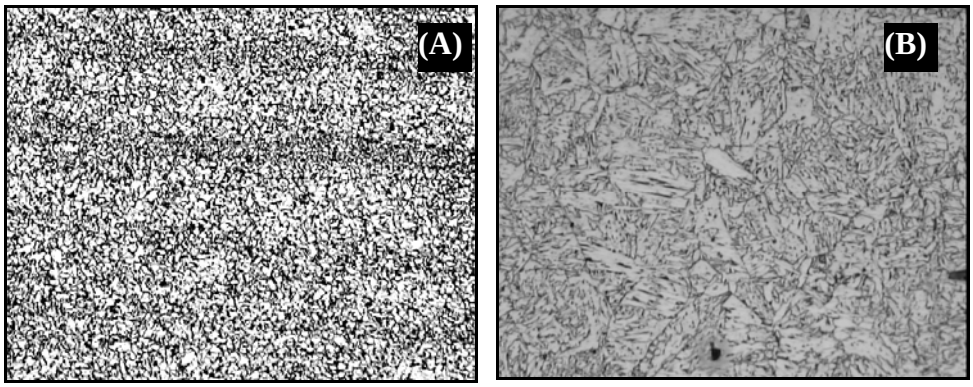


Figure 3. Microscope view of the HAZ of the steel (A) API X-65 and (B) API X-70 (200x).

Figure 1 shows a metallographic view of the base metal region of both steels where it can be observed a ferritic-pearlitic microstructure. However, for the API X-70 steel in figure 1B some regions without a clear microstructure definition can be seen, suggesting poor ferrite recrystallization during the thermo-mechanical process used to obtain this X-70 steel grade.

The welded metal region of both steels API X-65 and API X-70 (figures 2A and 2B, respectively) show an acicular ferrite configuration and primary grain boundary ferrite. However, the HAZ of both steels showed regions of coarse grains, with ferritic matrix with granular bainite and fine grains of ferrite-carbide aggregates, figures 3A and 3B.

### 3.2 – Fatigue crack propagation

Figures 4 and 5 presented the fatigue behavior of specimens submitted to overloads at $R$ = 0.1 and 0.5, respectively.

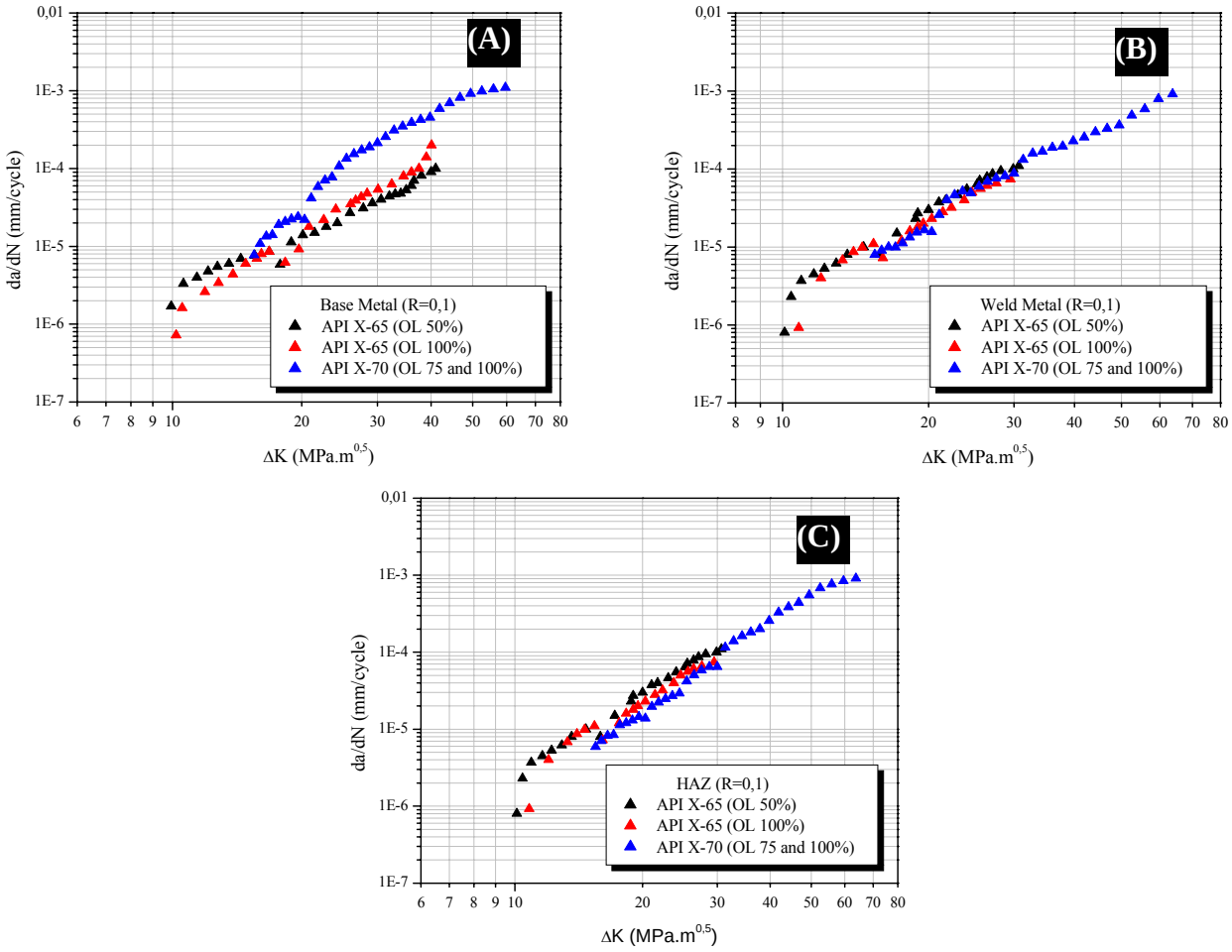


Figure 4. *da/dN* vs. Δ*K* curves for $R$ = 0.1 of API X-65 and API X-70 steels with overloads applications at regions: (A) base metal, (B) weld metal and (C) HAZ

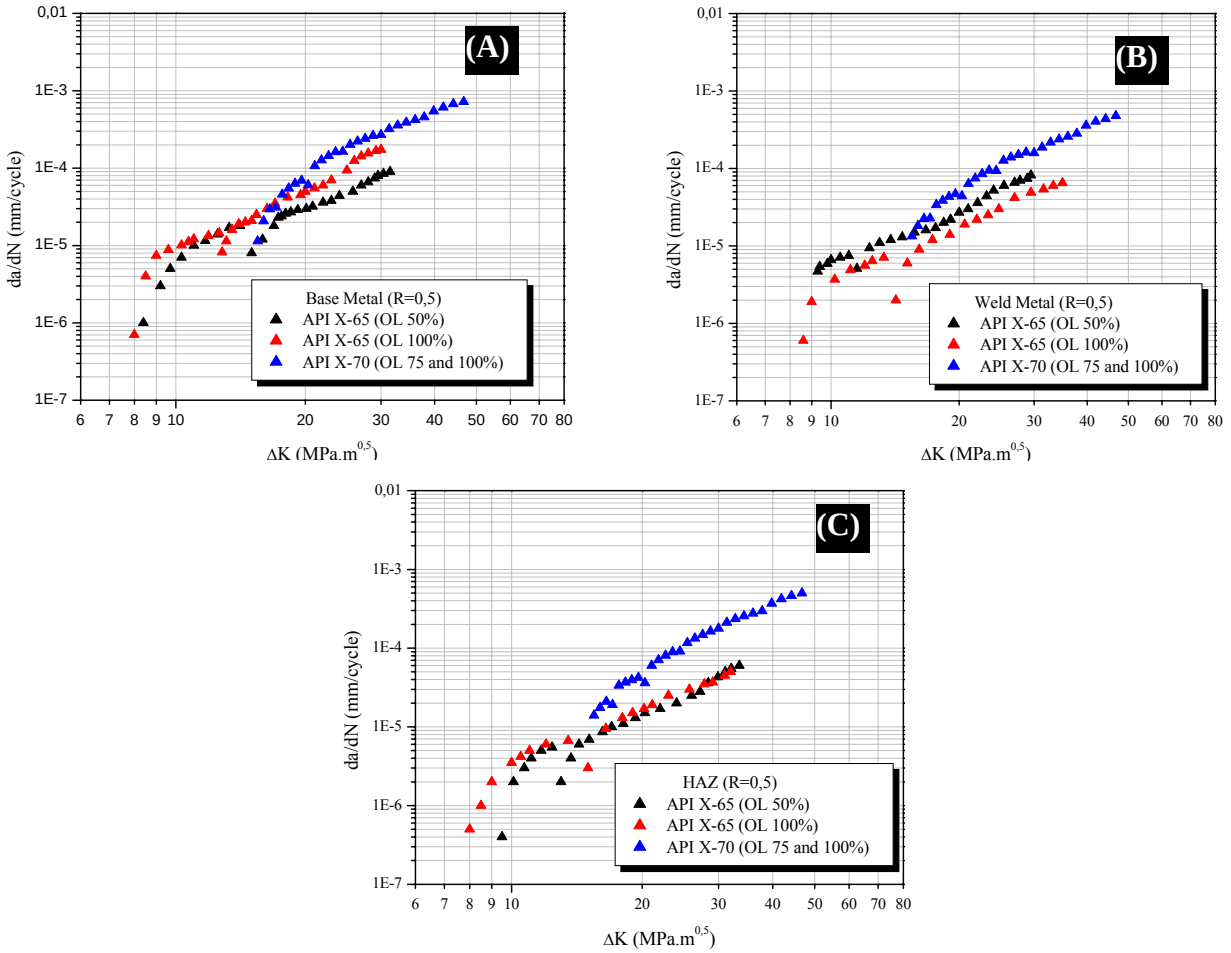


Figure 5. *da/dN* vs. Δ*K* curves for *R* = 0.5 of API X-65 and API X-70 steels with overloads applications at regions: (A) base metal, (B) weld metal and (C) HAZ

The results initially reveal that fatigue crack propagation in both steels was influenced by stress ratio. The base metal, weld metal and HAZ subjected to *R* = 0.5 showed the largest fatigue crack growth rates. It can be observed that the overload application in both cases promoted delays on crack growth rates. According to figure 4 and 5, the largest overloads promoted the greatest delays on crack growth at the three welded joints regions of API X-65 and API X-70 steels for *R* = 0.1. This behavior can be attributed to the absence or diminution of crack closure phenomena at high *R* values (Shuter and Geary, 1995).

In relation of the welded joint regions of API X-70 steel, the greatest delay on crack growth was also observed at the largest overload applied (100% of maximum load). Nevertheless, the delay effect in crack propagation with the subsequent overloads decreased with the increase of *ΔK* until a certain point (at elevated *ΔK* values, the overloads did not promote delays on the crack propagation). Geary (1992) says that the effective stress intensity factor is related to overload. In this sense, although no crack closure tests were performed, it is believed that the increase of *ΔK* during the propagation is responsible by approximating of the minimum stress to the crack closure stress, decreasing the delay caused by overload. When this stress is reached, the crack growth phenomenon is inexistent and, consequently, the crack propagation delay due to the overload did not occur.

In the welded joints of API X-65 steel, the overloads of 50% and 100% of maximum load promoted propagation rates very similar for *R* = 0.1 (figure 4). Comparing the behavior of base metal, weld metal and HAZ of API X-65 and API X-70 steels for the same stress ratio value, the results showed that the crack propagation rates of weld metal and HAZ with overload application presented the similar behavior, this effect being more pronounced in the weld metal.

In figure 5, for *R* = 0.5, the base metal presented the highest crack growth rate. Another observation is that the overloads promoted delays on crack propagation in all welded joint regions of API X-65 steel. The greatest delays on crack growth were observed at 100% of overload for the weld metal and HAZ. It can be verified that the crack growth rates in the HAZ were very similar. For the welded joints of API X-70 steel the results showed the same behavior presented by *R* = 0.1: the effect of crack propagation delay with the overloads decreased with the increase of *ΔK*.

The fatigue crack propagation rate is influenced by the material thickness that defines the predominance of plane stress state (thin materials) or plane strain state (thick materials) (Park *et al.*, 1996). In this case, the materials in the strain plane state shows the greatest crack growth rates (Branco *et al.*, 1999).

By comparison of the behavior in fatigue of both steels (figures 4 and 5), the results showed that the crack propagation rates of welded joints of API X-70 steel presented the greatest growth rates for all welded joint regions for $R = 0.5$ (thickness effect), differently of the behavior observed for $R = 0.1$ (no significative difference between weld metal and HAZ fatigue crack propagations), where the thickness effect was not observed. The welded joints of API X-70 steel experienced the smaller effect of overloads than welded joints of API X-65 steel, provably due to higher plane strain condition and smaller plastic zone size formed by overload than that of the thinner material (API X-65).

No residual stress measurements were carried out. However, it has been known that the tensile and compressive residual stresses at the welded joints increase and decrease the crack propagation rates, respectively. Therefore, the crack growth behaviour presented in this work could have been influenced by the presence of these residual stresses.

## 4 – Conclusions

The results of the present study support the following conclusions:

1 – The overloads promoted delays on the fatigue crack propagation in the welded joints of both steels;

2 – The greatest delay on crack propagation was observed with the greatest overload;

3 – The delay on the fatigue crack growth of welded joints of API X-70 decreased with the increase of $\Delta K$;

4 – In both steels, the crack propagation rates of weld metal and HAZ with overloads showed similar behavior for $R = 0.1$. For $R = 0.5$, the welded joint regions of API X-70 steel showed the greatest crack growth rates;

5 – The welded joints of API X-70 steel experienced smaller effect of overloads than welded joints of API X-65, for both $R$ values.

## 5 – Acknowledgements

The authors would like to thank to PETROBRAS, CONFAB, GM/CETEx, CNPq CT Petro (process number 502084/03-0) and CAPES for financial support.

## 6 – References

ASTM E399, 1999, Standard Test Method for Plane-Strain Fracture Toughness of Metallic Materials.

ASTM E647, 1999, Standard Test Method for Measurement of Fatigue Crack Growth Rates.

Branco, C.M., Fernandes, A.A. and de Castro, P.M.S.T., 1999, "Fadiga de Estruturas Soldadas", Fundação Calouste Gulbenkian, Lisbon, Portugal, 902 p.

BS 6835, 1988, Determination of the Rate of Fatigue Crack Growth in Metallic Materials.

Geary, W., 1992, "A Review of Some Aspects of Fatigue Crack Growth Under Variable Amplitude Loading", International Journal of Fatigue Vol. 14, No. 6, pp. 377 – 386.

Maddox, S. J., 1998, "Fatigue Performance of Large Girth Welded Steel Tubes", Proceedings of 17th OMAE 98, July 5 – 7, Lisbon, Portugal, ASME.

Park, H-B., Kim, K-M., Lee, B-W., 1996, "Plastic Zone Size in Fatigue Cracking", Int. J. Pres. Ves. & Piping, Vol. 68, pp. 279 – 285.

Shuter, D. M., Geary, W., 1995, "The Influence of Specimen Thickness on Fatigue Crack Growth Retardation Following an Overload", International Journal of Fatigue Vol. 17, No. 2, pp. 111 – 119.

Zhao, M. C., Yang, K., Shan, Y-Y., 2002, "The Effects of Thermo-mechanical Control Process on Microstructures and Mechanical Properties of a Commercial Pipeline Steel", Materials Science and Engineering A, Vol. 335, pp. 14 – 20.

## 7 – Responsibility notice

The authors are the only responsible for the printed material included in this paper.